J Mater Sci
DOI 10.1007/s10853-011-6242-9

Multiscale micro-patterned polymeric and carbon substrates derived from buckled photoresist films: fabrication and cytocompatibility

Manish M. Kulkarni · Chandra S. Sharma · Ashutosh Sharma · Sushma Kalmodia · Bikramjit Basu

Received: 1 October 2011 / Accepted: 27 December 2011

Abstract We report here a novel and simple buckling-based multiscale patterning of negative photoresist films which were subsequently pyrolyzed to yield complex micro-patterned carbon surfaces. Unlike other polymers, the use of a photoresist layer allows the overall pattern definition by photolithography on which the geometry and length scale of the buckling-instability are superimposed. The photoresist film swells anisotropically during developing and buckles after subsequent drying due to the difference in the shrinkage of the hard cross-linked layer on top of a softer native pre-polymer. We studied the conditions for the formation of a wide variety of complex, fractal buckling patterns as well as directionally aligned zigzag patterns over a large area. For example, the buckling diminished for the films below a critical thickness and after a prolonged UV exposure, both of which eliminate the softer under-layer. These patterned carbon substrates are also shown to be biocompatible for the cellular adhesion and viability by using L929 mouse fibroblast cells, thus indicating their potential use in bio-MEMS platforms with a conductive substrate. The buckled carbon patterns were found to be a better choice of a substrate for cell growth and viability as compared to flat and simply periodic patterned carbon surfaces.

M. M. Kulkarni
Department of Polymer Engineering, The University of Akron, Akron, OH 44325, USA

C. S. Sharma
Department of Chemical Engineering, Indian Institute of Technology, Hyderabad, Yeddumailaram 502205, Andhra Pradesh, India

A. Sharma (✉)
Department of Chemical Engineering & Unit on Nanosciences, Indian Institute of Technology, Kanpur 208016, Uttar Pradesh, India
e-mail: ashutos@iitk.ac.in

S. Kalmodia · B. Basu
Department of Materials Science and Engineering, Indian Institute of Technology, Kanpur 208016, Uttar Pradesh, India

Introduction

Buckling is commonly observed in bilayers when a hard top skin layer on a relatively thick soft bottom layer undergoes compression beyond a critical limit [1]. This buckling phenomenon is observed in various systems, including metal-on-polymer [2], gels [3], composites [4], and polymer-multilayer [5]. Buckling in films was initially thought as undesirable, and efforts were made to avoid it, particularly in polymeric thin films until Whitesides et al. [6] demonstrated that by controlling the stress points and elastic moduli of the system, spontaneously self-assembled as well as high fidelity periodic patterns can be generated. Recently, it was shown that the periodicity of the buckled patterns can be used as a measure of film's elastic modulus [7, 8].

Here, we report spontaneous formation of buckling patterns during processing of UV exposed negative photoresist films. In this study, the buckling of a photoresist material in a controlled fashion has been used as a novel tool to generate multiscale polymer and carbon micro-patterns which allows a combination of top-down (photolithography) and bottom-up self-organization to define intricate patterns. The use of a photosensitive material which was not penetrated throughout its thickness uniformly thus forms a bilayer which allows the buckling to occur during developing. The buckling of a directly photo-patternable material is used as a novel tool to generate

Published online: 10 January 2012

intricate multiscale polymer and carbon micro-patterns by a combination of top-down (photolithography) and bottom-up self-organization. An overall micro-pattern that subsequently undergoes buckling is easily defined first by photolithography and subsequent buckling adds a second geometry and length scale to the master pattern. Use of a photoresist allows direct integration of this method in the MEMS technology to create multiscale patterns. Another motivation for the use of this photoresist material is the formation of carbon structures upon pyrolysis. Once the photoresist surface is patterned by integration of photolithography and self-organized buckling to create large area multiscale structures, same can be converted to carbon structures by pyrolysis. We thus demonstrate a novel and simple approach based on controlled buckling in the photoresist films to prepare multiscale micro-patterned polymeric and carbon surfaces. These micro-patterned carbon surfaces are also tested for cell viability with a view toward applications in bio-MEMS platforms.

Carbon is a preferred material for a large number of applications owing to its wide electro-chemical stability, biocompatibility, and chemical inertness [9]. Conventional carbon microfabrication technologies like focused ion beam, reactive ion etching, and printing [10] are time consuming, expensive, and limited to small areas. Soft lithographic techniques to obtain glassy carbon microstructure by patterning a resin in an elastomeric mold followed by pyrolysis have also been reported [11]. Another emerging microfabrication technique for carbon is based on the thermal pyrolysis of patterned photoresists [9], [12–16]. Usually, the negative SU-8 and positive AZ4330 photoresist-based patterned structures retain their shape during pyrolysis. This technology has recently attracted a lot of interest because at different pyrolysis conditions (e.g., different pyrolysis temperature), the pyrolyzed photoresist or polymer can be converted to different types of carbon with different specific gravity, resistivity, and crystalline structures (e.g., glassy carbon and graphitic carbon). Most of the techniques mentioned above are suitable for preparing regularly shaped periodic patterns. Here, we present a new method to generate carbon surfaces with unconventional multiscale structures such as periodic zigzag sinusoidal channels as well as fractal patterns based on buckling of a negative photoresist.

Further, we study cytocompatibility of the patterned carbon surface by in vitro cellular biocompatibility of L929 fibroblast cell line by cell adhesion and cell viability (MTT) assessment and thus show that the buckled patterns are more suited for cell-compatibility. Cell adhesion on a substrate is dependent on many parameters such as surface topography, porosity, and surface molecules. In the present investigation, random buckling induced patterned carbon surfaces were used for the support and guidance of the cellular orientation through cytoplasmic extension and attachment of extra cellular matrix (ECM) associated molecules for the initial cell attachment [17].

Experimental section

Preparation of buckling induced patterned films

Xylene diluted SC-100 (a conventional cyclic polyisoprene photoresist produced by Olin Hunt Co. under the designation WayCoat SC-100) negative photoresist was spin coated on Si-wafers to obtain film thicknesses (h) in the range of 2.5 to 5.5 μm by varying the spin speed and concentration of photoresist in xylene. The films were then exposed to UV light for different time intervals in two different ways: first as flood exposure without any mask and second, using a SF-100 photolithography unit (Intelligent Micropatterning, CA), which selectively exposed parts of the film through a digital mask. The UV radiation cross-linked the exposed part of the negative photoresist. The UV exposed films were then developed in xylene. During this step, the top hard cross-linked layer and the softer native pre-polymer at bottom swell anisotropically and the photoresist film buckles when the film is dried in air due to the unequal shrinkage of these two layers. The photoresist films were then dried in flowing N_2 gas at room temperature (25 °C). This experimental protocol is shown schematically in Fig. 1.

The patterned photoresist films were then pyrolyzed in a furnace under optimized conditions such that the carbonized film retains the buckling patterns in carbon. Before pyrolysis, a quartz tube was purged with nitrogen gas at a 0.5-L/min flow rate for about 20 min to remove unwanted air or oxygen. The heating rate was fixed at 5 °C/min, and the N_2 gas flow rate was kept constant at 0.2 L/min during heating. Once the maximum temperature was reached, it was maintained for 60 min. The furnace was then cooled to room temperature slowly over duration of 10 h in flowing N_2 gas to obtain carbon films.

Cell culture tests

In this study, mouse fibroblast cells (L929) were used for cytotoxicity and cellular study. The cryo-vial was rapidly thawed and cultured in Dulbecco's modified Eagles medium (DMEM), supplemented with 10% serum (Sigma Aldrich), 1% antibiotic cocktail (10,000 IU penicillin 10 mg streptomycin and 25 μg amphotericin B/mL) (Sigma Aldrich) at 37 °C temperatures in 5% CO_2 humidified atmosphere. The sub-confluent monolayer was trypsinized using 0.5% trypsin and 0.2% EDTA solution (Sigma Aldrich). The exponentially growing cells were used to study cellular behavior and viability.

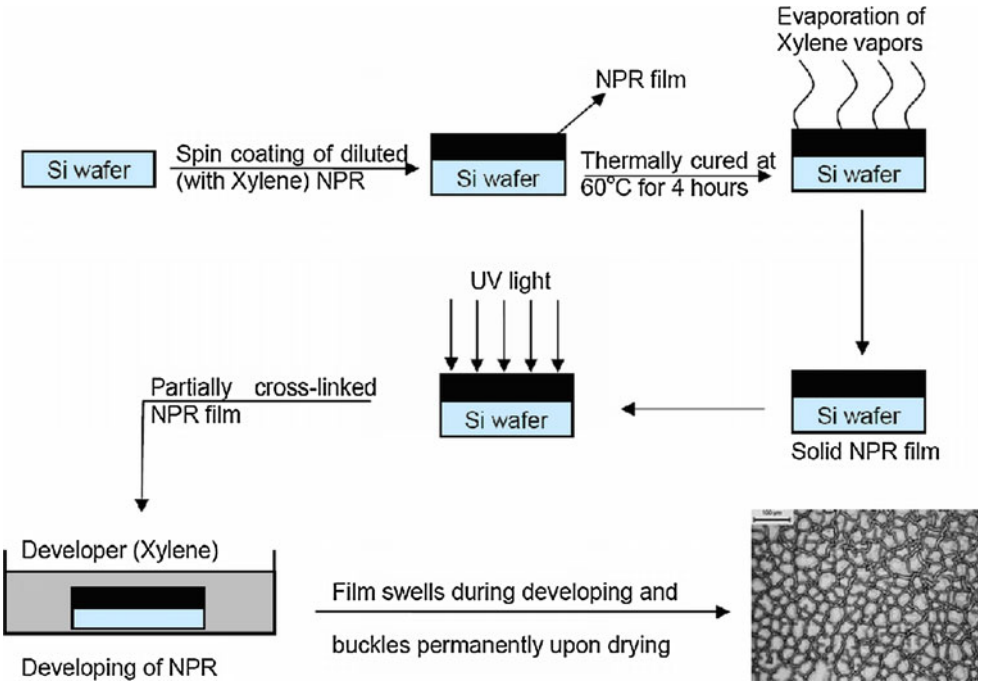

Fig. 1 Experimental protocol to prepare buckled patterns in photoresist film

Cellular behavior

L929 fibroblast cells were seeded on selected samples and control (gelatin coated polymeric disc) at cell density $\sim 5 \times 10^3$ in six well plate, and cellular behavior was studied after the 48 h of seeding. The cell density was measured by Haemocytometer (improved Neubauer, depth 0.1 mm). After 48 h of seeding, the culture medium was removed from each well and cells were fixed with 2% glutaraldehyde in PBS for 30 min on the samples. The adhered cells on the control cover slip and carbon substrate were dehydrated twice using a series of ethanol solutions (30, 50, 70, 90, and 100%) for 10 min by each dilution level and then further dried using hexamethyldisilazane (HMDS, Sigma). The dried samples were sputter coated with gold, and detailed analyses of cell adhesion and morphology were carried out using SEM (SUPRA 40 VP, Gemini, Zeiss).

Mitochondrial activity

Cell viability of seeded cell on carbon substrate as well as control samples were assessed by the MTT assay, according to the method of Mosmann et al. [18]. First, the L929 cells were seeded in six well plates at density of $\sim 5 \times 10^3$ on control polymer disc and samples followed by incubation for 3 and 5 days, respectively. After incubation for a fixed time, the samples were washed with 1× PBS, and 10 µL of MTT (5 mg/mL)/100 µL DMEM was added in each well in-between image acquisition in-phase contrast microscope for the formation of the formazan crystal. Thereafter, MTT solution was carefully removed and washed with 1× PBS. Later, formazan crystals were solubilized by adding 200 µL of DMSO. Subsequently, the complete violet color solution was transferred into the 96 well plate, and mitochondrial activity of the viable cells was quantified by measuring by ELISA automated microplate reader (Bio-Tek, model ELx800).

Results and discussion

Although, a negative photoresist crosslink upon exposure to UV, the UV penetration along the thickness is observed to be slow for the negative photoresist chosen. Also, as the top layer of the film crosslinks, the UV transparency of the film possibly decreases. As a result, when the film was exposed for short periods, a "bilayer" structure forms in the film with a top crosslinked hard layer on a soft un-crosslinked bottom layer. After exposure, when the film is developed in xylene, extent of swelling for these two layers is significantly different from each other and subsequently when the film is dried in air, the compression forces yield buckling patterns. Buckling induced patterns in the top layer of the film approach freeze as shown in Fig. 2.

Figure 2 shows evolution of buckling patterns observed in NPR film as a function of UV exposure time. As seen from Fig. 2a, small semi-circular buckling patterns developed even for short UV exposure of 5 s indicate that the top layer of the film crosslinks very quickly. These patterns start growing on increasing the exposure time to 7 s as observed in Fig. 2b. As the UV exposure time is increased up to 10 s,

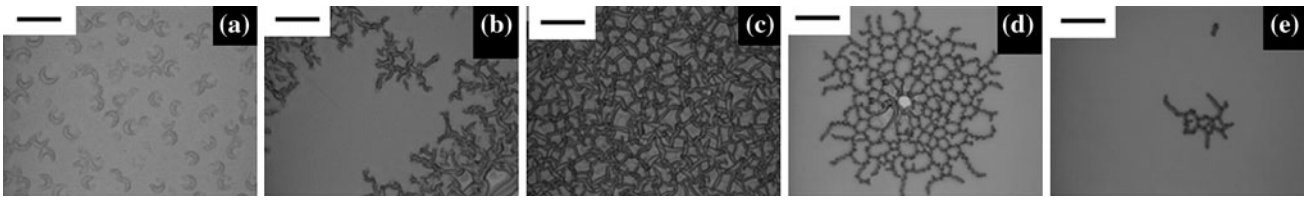

Fig. 2 Optical micrographs showing buckling in 5.5 μm thick NPR films as a function of flood UV exposure time, **a** 5 s; **b** 7 s; **c** 10 s; **d** 15 s; and **e** 20 s (*scale bar*: 100 μm)

complex arc-filling network-like buckling patterns were observed, as shown in Fig. 2c. Interestingly, further increase in the time of exposure decreased buckling. At 15 s long UV exposure, very few regions on the film surface with buckling were observed (Fig. 2d). These buckled regions decreased further in size and number at 20 s UV exposure (Fig. 2e). These results are consistent with the bilayer mechanism where a hard layer buckles over a soft partially cross-linked film. Buckling is not observed if the film is exposed for a sufficiently longer time since the film crosslinks uniformly across the whole thickness (For 5.5 μm thick films, no buckling was observed for exposure time longer than 20 s.).

A similar effect of uniform crosslinking along the thickness of the NPR film was verified by decreasing the film thickness and keeping the UV exposure time constant at 15 s. As seen from three-dimensional (3D) AFM topographical images of the NPR films shown in Fig. 3, buckling diminish quickly with decrease in the film thickness from 5.5 to 2.5 μm.

The buckling patterns as obtained upon flood exposure for a fixed film thickness of the photoresist film were also characterized using Gwyddion and radial profile plots in ImageJ (Image processing and analysis in Java) software. These results are summarized in Fig. 4, and the values of dominated wavelength are tabulated below (Table 1).

As observed from Fig. 4 and Table 1 that the dominant periodicity of the buckled patterns for a 5.5-μm thick photoresist film increased from 1 to 28 μm with increase in UV exposure time from 5 to 20 s. It is consistent with the results obtained as buckling disappears (infinite wavelength) for exposure time longer than 20 s.

A unique advantage of the UV sensitive nature of the NPR films is that by controlling the UV exposed areas of the film, buckling patterns can be tuned and forced to align along a specific direction. NPR films were exposed to pattern UV light using a digital mask SF-100 photolithography unit. The aim here was to expose NPR film under UV fringe pattern, and buckling was studied as a function of the UV fringe width and exposure time. Figure 5 shows the buckled patterns of the NPR film exposed to an alternating dark and UV radiation band of 15 μm for different time intervals.

Figure 5 shows that at lower exposure time (Fig. 5a), the buckling occurs only along the UV exposed channels. However, the wavelength of buckling is not uniform and varies from 17 to 25 μm along the channel. No long range in-phase or out-of-phase zigzag pattern in neighboring lines could be observed in Fig. 5a. Interestingly, a 10-s exposure produces periodic in-phase meandering of neighboring lines to produce undulating channels as seen in Fig. 5b. However, as the exposure time increases to 15 s, the buckled lines start to "cross-talk" to neighboring lines through the residual layer (Fig. 5c) to produce periodically bridged parallel lines. After 20 s exposure (Fig. 5d), the buckling loses almost all of 1D alignment and becomes

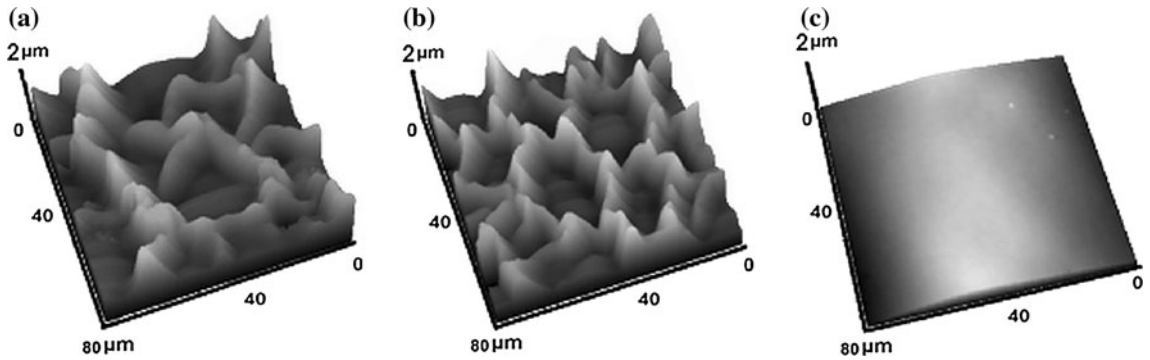

Fig. 3 AFM 3D topography images showing buckling in SC-100 photoresist exposed for 15 s in UV as a function of thickness: **a** 5.5 μm; **b** 4.0 μm; and **c** 2.5 μm

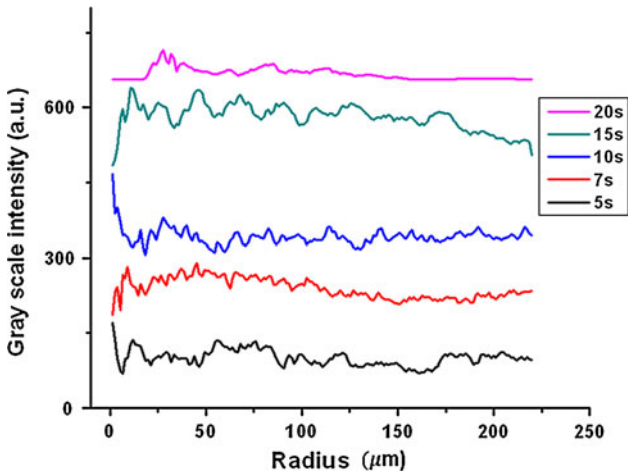

Fig. 4 Gwyddion and radial profile plots showing the dominant wavelength of buckling induced patterns for a 5.5-μm thick photoresist film as shown in Fig. 2

Table 1 Dominant peak position with different UV exposure time for a 5.5-μm thick photoresist film (corresponds to Fig. 4)

UV exposure time (s)	Peak position (μm)		
	First peak	Second peak	Third peak
5	1.0*	12.0	15.0
7	4.0*	6.6	9.3
10	4.0*	16.0	21.0
15	6.6	12.0*	17.3
20	22.6	28.0*	32.0

* Indicates dominating periodicity

progressively similar to a uniform UV exposure. Transition to a 2D-regime of buckling may be owing to significant UV light scattering in the unexposed parts of film and the growth of stiffened top layer which makes buckling harder without any mass redistribution in the under-layer. Similar to the case of uniform UV exposure, no buckling was observed after very long exposure times (>50 s).

Figure 6 shows the 3D AFM topographic images corresponding to buckling patterns obtained by exposing NPR film to UV through an equidistant 15-μm fringe pattern as a function of film thickness. UV exposure time in all the cases reported here is 15 s. For 2.5 μm thick film, buckling gets diminished in lateral direction (Fig. 6c) supporting the mechanism discussed above. It is to be noted here that buckling patterns are observed to be hierarchical in nature. The optical micrograph for this case (Fig. 7) fails to resolve the small scale buckling features as apparent in Fig. 6c.

As mentioned above, no buckling in lateral direction was observed for 2.5 μm thick films for 15 μm fringe patterns as seen from Fig. 7. For 2.5 μm thick films, the unexposed parts were nearly washed away exposing the substrate during the developing of the film. The exposed and unexposed channel widths are non-uniform, indicating side-wise UV scattering inside the non-exposed parts of the films. Again, the lack of residual unexposed soft layer between two adjacent exposed channels and comparatively large depth of stiffened top layer led to suppression of buckling.

In the next step, the films were exposed to UV fringe patterns of increasing fringe width. This study determines the critical fringe width necessary to maintain the forced (zigzag) alignment of buckled patterns along the UV exposed part of the film. Figure 8 shows buckling patterns in the 5.5-μm thick NPR film, when the fringe width was varied from 30 to 225 μm with a constant exposure time of 10 s.

As seen from Fig. 8, the zigzag alignment of the buckled patterns markedly decreases as the fringe width is increased from 15 to 30 μm (Fig. 8a). The patterns remain loosely aligned with further increase in fringe width (Fig. 5b,c) and give way to completely random buckling patterns confined to the exposed part at 225 μm fringe width (Fig. 5d). At 225 μm, the patterns within the exposed domains resemble to that of a flood UV exposure (Fig. 2c). Hence, it can be concluded that critical fringe width of forced alignment of the buckled patterns is smaller than 30 μm.

Given the polymeric nature of the films and hierarchical buckling patterns of micron length scale, it can be envisioned that carbonization of the films may yield substrates for cell adhesion and growth. The patterned carbon surfaces mimic more closely in structural design with the extracellular matrix and promote the cell growth and

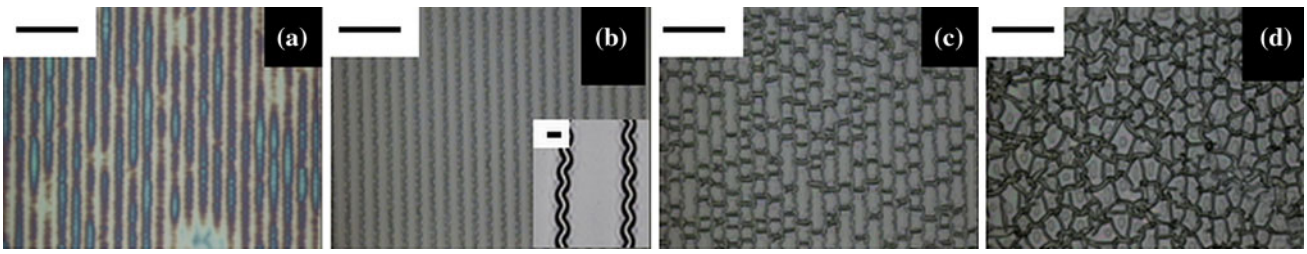

Fig. 5 Optical micrographs revealing buckled patterns of 5.5 μm thick NPR film exposed to UV through an equidistant 15-μm fringe pattern for different time intervals: **a** 5 s; **b** 10 s; **c** 15 s; and **d** 20 s (*scale bar:* 100 μm). The *inset* shows high-magnification image of aligned buckling pattern (*scale bar* for *inset* image: 10 μm)

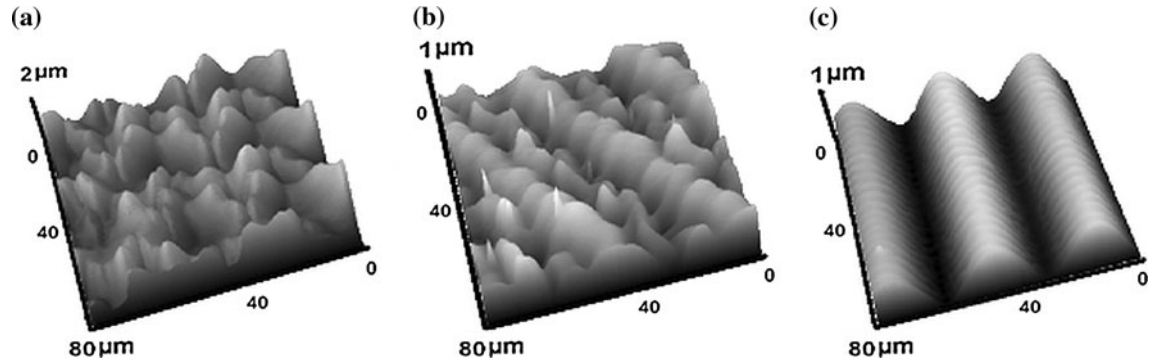

Fig. 6 The 3D AFM topographic images of buckling patterns through an equidistant 15-μm fringe pattern as a function of thickness of the NPR film: **a** 5.5 μm; **b** 4.0 μm; and **c** 2.5 μm. UV exposure time in all the cases was 15 s

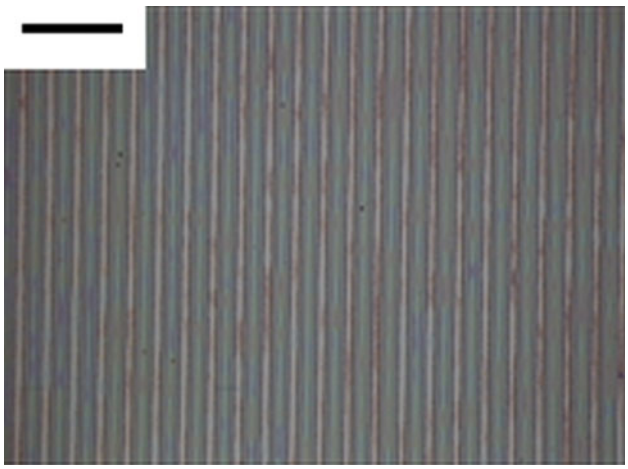

Fig. 7 A 2.5-μm thick NPR film after exposure to 15 μm UV fringe pattern for 15 s and developing. The unexposed parts of the film wash away completely during developing the substrate. (*Scale bar:* 100 μm)

viability. Hence, the buckled NPR films were carbonized by heating at 900 °C in an inert atmosphere. It was observed that under optimized conditions (see "Experimental" section for details) of N_2 flow and heating and cooling rate, the buckled patterns preserved their shape and fidelity. Figure 9a–b shows carbonized surfaces of NPR films exposed to UV through an equidistant 45 μm fringe pattern and flood UV exposure, respectively.

These buckling-based micro-patterned carbon surfaces were used further to test the cytocompatibility using L929 mouse fibroblast cells as discussed below.

Cellular behavior

In order to study the influence of material surface and composition on the cell morphology and proliferation, the cellular cytoplasmic extension in the form of filipodium and lamilipodium was carefully studied using SEM images with respect to the cell morphology on control material (cell seeded on glass slide). One can use the fluorescence microscopy analysis also for the morphological analysis that also gives the same information that we obtained from the SEM images. Higher magnification SEM images of L929 cells after treatment of 24 h of seeding on different substrates are shown in Figs. 10 and 11, respectively. The cellular morphology on the patterned nanostructure carbon surface shows filopodia and lamelipodium. An earlier study on the role of the lamellipodium in cell migration concluded that actin monomer assembly is required for the cell lamellipodium outgrowth in the migratory cells [17]. Nevertheless, the observation of larger elongated cell is clearly observed even in the smooth surface, but the growth pattern of the cell is also different. Cytoplasmic extension is less prominent in the case of the smooth and control surface (Figs. 10a, 11a, b). The cell-to-cell contact was clearly observed in the case of patterned

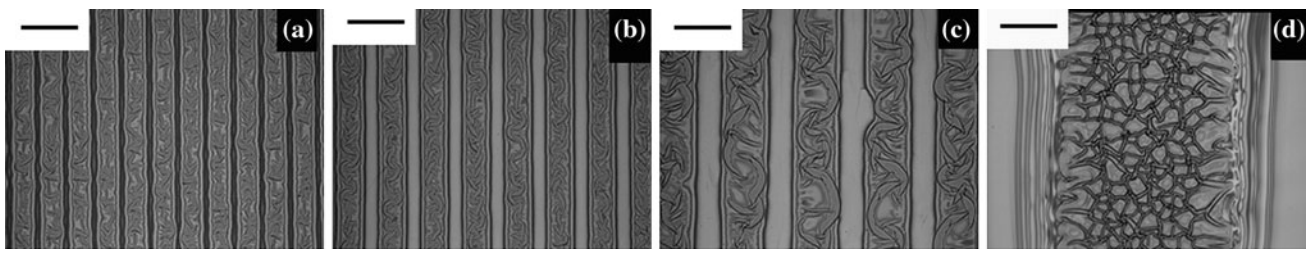

Fig. 8 Buckling patterns observed in 5.5 μm thick NPR film when the fringe width was varied from **a** 30 μm; **b** 45 μm; **c** 75 μm; and **d** 225 μm (*scale bar:* 100 μm). Exposure time was 10 s for all the cases

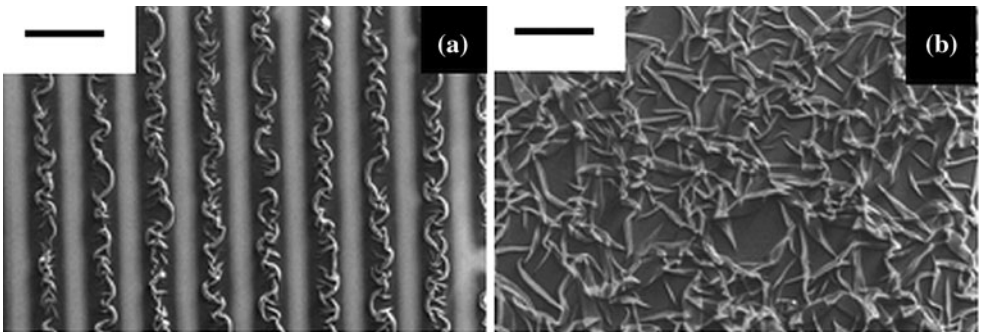

Fig. 9 Scanning electron micrographs of buckled patterns of NPR film carbonized at 900 °C **a** exposed to UV through an equidistant 45 μm fringe pattern and **b** flood UV exposure. *Scale bar:* 100 μm)

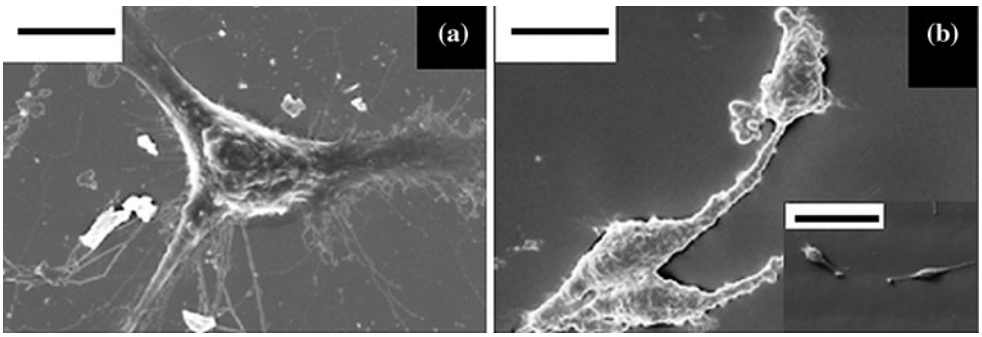

Fig. 10 Cell spreading on **a** control and **b** photoresist derived patterned carbon surfaces (*scale bar:* 2 μm). *Inset* shows lower magnification image of (**b**) (*scale bar* for *inset* image: 20 μm)

photoresist carbon substrate (Figs. 10b, 11c), which suggests that the patterned surfaces provide an orientation to the cells that support cell substrate and cell-to-cell communication.

Cytotoxicity

It is well known that MTT reagent directly reacts with the mitochondria (mitochondrial dehydrogenase) of metabolically active cells [18]. Cell viability analyzed by the MTT assay is a quantification of the cell proliferation through mitochondrial dehydrogenase enzyme of the live cells. MTT reacts with the enzyme and form formazen crystal. The % of cell viability was calculated through the optical density of the blue color of formazen crystal that dissolved by DMSO. The % cell viability is directly correlated with the cell proliferation. Mouse fibroblast cells (L929) were seeded on control disc and various carbon substrates. Figure 12 shows results of the cell viability after the 3 and 5 days of fibroblast culture on carbon smooth surface and pattern surface with respect to the control material. An analysis of MTT data of patterned and smooth surfaces reveals a maximum of 99.9% of viability after 5 days of culture in the case of patterned surface. In contrast, smooth surface shows a reduction in the viability from 77.4 to 68.4% with an increase in culture duration from 3 to 5 days. Increased % viability of L929 cells on the buckled

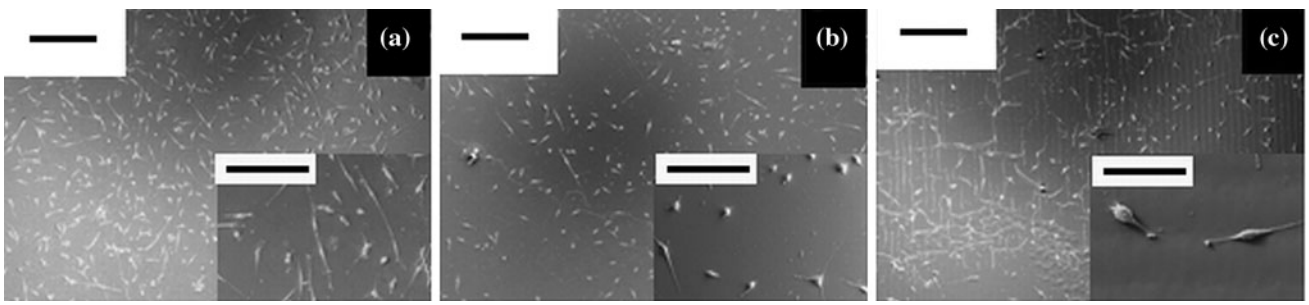

Fig. 11 SEM micrographs showing the cell (L929 Mouse Fibroblasts) adhesion after 24 h of seeding on various surfaces **a** control; **b** smooth; and **c** patterned carbon (*Scale bar:* 100 μm). Higher magnification images are added as *inset* (*scale bar:* 20 μm)

surface shows that the patterned carbon surface was more helpful for the growth and viability of cells. It is possible that patterned surfaces provide higher surface area as compared to the smooth surface for enhanced cellular functionality. Moreover, the micrometer size of buckling carbon substrate shows a better topography for the cell attachment and extracellular molecules attachment. In view of the fact that L929 fibroblast cell is a connective tissue cell, such cells exhibit good cell–cell contact by extracellular matrix. As the statistical analysis of the cytotoxicity data at $p < 0.05$ could not reveal any significant difference in the cell viability with respect to the control material, it can be concluded that photoresist derived carbon surface (smooth as well as patterned) does not show chemical cytotoxicity. Moreover, after 5 days of cell culture on the photoresist derived carbon substrate in the presence of protein (FBS) containing DMEM, the resistance of material against fouling could be observed [19]. The cytocompatibility of the pattern photoresist carbon surface can therefore be confirmed as % viability which is much higher after 5 days of culture on the pattern surface compared to smooth surface.

It may be noted that the patterned carbon surface mimics more closely in structural design with the ECM and promote the cell growth and viability, as compared to the smooth surface. This observation that patterned surfaces influence the cellular responses is also supported in literature [20–22]. The initial cell attachment to the substrate occurs through integrin, a transmembrane protein present on the cell. The patterned surfaces influence the assembly of specific type of integrin proteins. The cytoplasmic side of the integrin link to the cytoskeleton that effects the gene expression through up- and down-regulation of specific gene and that indirectly regulates the ECM molecules [20, 21]. The ECM component closely mimics, in terms of diameter, with the patterned carbon surface. Moreover, the pattern surfaces modulate the cell orientation, cell structure, cytoskeleton reorganization, and ECM protein deposition on the tailored surfaces [22]. Extracellular components such as collagen, fibronenctin help in cellular adhesion through creating the microstructure in the initial stage of the cell attachment. However, the substrate adhesion molecules and surface topography contributed to dynamics of cell−ECM interactions that contribute to cell migration, proliferation, division, differentiation, and programmed death, which are indispensible for the successful and long-term cell biomaterial interactions [23]. Therefore, the tailored surface for the growth of the connective tissue cell line like L929 fibroblast easily interfaces on the patterned carbon surface and support cell growth and migration through reversible attachment of cells on the surface [24, 25].

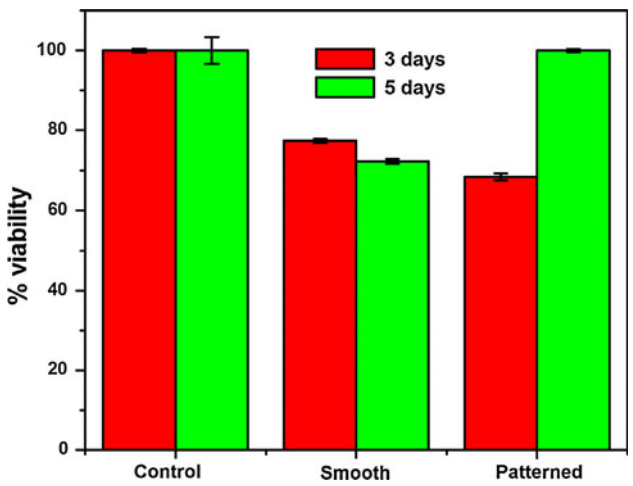

Fig. 12 Cell viability as shown by MTT assay results after 3 and 5 days of cell culture on control, smooth carbon surface, and patterned carbon surface

Conclusions

We have shown that a negative photoresist layer forms buckling patterns when UV exposed for a short duration depending on its thickness and then developed in a solvent. A short exposure develops a gradient of cross-linking and hardness across the film thickness, which allows buckling of the hard over-layer on top of a soft under-layer. Combination of a top-down method (photolithography) with self-organized buckling allows generation of a multi-scale surface pattern where buckled structures are superimposed on the domains defined by lithography. For a given thickness film, an optimal intermediate exposure time produced space-filling network-like buckled patterns, but much shorter or longer exposure both diminished the extent of buckling. The geometry of buckled patterns could be modulated by changing the exposure time, film thickness, and lateral confinement (width of UV exposed regions). Thus, some unconventional patterns such as zigzag channels and other complex multiscale patterns could be produced. Further, it is shown that these patterned surfaces could be pyrolyzed at high temperature under optimized conditions to yield micro-patterned carbon substrates that were tested for their cytocompatibility. Our study confirms the absence of any significant cytotoxic effect of photoresist-derived carbon substrates to L929 cells. The study also points toward the fact that the surface topography can influence the cell viability. The patterned carbon surfaces are assessed to be the better substrates to support enhanced cellular proliferation and long-term cell viability.

Acknowledgement This study is supported by the DST Unit of Excellence on Soft Nanofabrication, IIT Kanpur, and by an IRHPA grant from the DST.

References

1. Genzer J, Groenewold J (2006) Soft Matter 2:310
2. Bowden N, Brittain S, Evans A, Hutchinson J, Whitesides GM (1998) Nature 93:146
3. Sultan E, Boudaoud A (2008) J Appl Mech 75:051002
4. Lankford J (1995) J Mater Sci 30:4343. doi:10.1007/BF00361515
5. Hyun DC, Moon GD, Park CJ, Kim BS, Xia Y, Jeong U (2010) Adv Mater 22:2642
6. Bowden N, Huck WT, Paul KE, Whitesides GM (1999) Appl Phy Lett 75:2557
7. Amis E, Karim A, Stafford CM, Harrison C, Beers KL, Van-Landingham MR, Kim H, Volksen W, Miller RD, Simonyi EE (2004) Nat Mater 3:545
8. Fasolka MJ, Wilder EA, Lin-Gibson S, Guo S, Stafford CM (2006) Macromolecules 39:4138
9. Wang C, Madou M (2005) Biosens Bioelectron 20:2181
10. Madou MJ (2002) The science of miniaturization, 2nd edn. CRC Press, Boca Raton
11. Schueller OJ, Brittain ST, Whitesides GM (1997) Adv Mater 9:477
12. Ranganathan S, Mccreery R, Majji SM, Madou MJ (2000) Electrochem Soc 147:277
13. Wang C, Zaouk R, Park B, Madou M (2008) Int J Manuf Tech Manag 13:360
14. Wang C, Jia G, Taherabadi LH, Madou MJ (2005) J MEMS 14:348
15. Wang C, Taherabadi L, Jia G, Madou M, Yeh Y, Dunn B (2004) Electrochem Solid State Lett 7:A435
16. Teixidor GT, Gorkin RA, Tripathi PP, Bisht GS, Kulkarni M, Maiti TK, Battcharyya TK, Subramaniam JR, Sharma A, Park BY, Madou M (2008) Biomed Mater 3:034116
17. Louise PC (1999) Curr Bio 9:1095
18. Mosmann TJ (1983) Immunol Methods 65:55
19. Lee J, Chu BH, Chen K, Ren F, Lele TP (2009) Biomaterials 30:4488
20. Anselme K, Davidson P, Popa AM, Giazzon M, Liley M, Ploux L (2010) Acta Biomater. doi:10.1016/j.actbio.2010.04.001
21. Pennacchi M, Armentano I, Zeppetelli S, Fiorillo M, Guarnieri D, Kenny JM, Netti PA (2004) Eur Cell Mater 7:77
22. Petreaca MM (2008) In: Atala A, Lanza R, Thomsan JA, Nerem R (eds) Principles of regenerative medicine, 5th edn, Academic Press, p 66
23. Albert B, Johnson A, Lewis J, Raff M, Roberts K, Walter P (2002) Garland Science Group, 4th edn. Taylor and Francis, New York
24. Misra A, Pei ZLR, Wu Z, Thirumaran T (2007) Biomed Biophys Comm 364:908
25. Detrait E, Lhoest JB, Knoops B, Bertrand P, Aguilar PVB (1998) J Neurosci Methods 84:193